J Mol Model (2001) 7:378–383
DOI 10.1007/s00894-001-0053-x

ORIGINAL PAPER

Igor Z. Zubrzycki · Gregory L. Blatch

DFT study of a substrate and inhibitors of 1-deoxy-2-xylulose-5-phosphate reductoisomerase – the potential novel target molecule for anti-malaria drug development

Received: 5 June 2001 / Accepted: 6 September 2001 / Published online: 27 October 2001

Abstract 1-Deoxy-2-xylulose-5-phosphate (DOXP) reductoisomerase is a novel target for developing anti-malaria drugs. The determination of structural and electronic properties of the inhibitor molecules is of crucial importance for analyzing the interactions between DOXP-reductoisomerase and its inhibitors. Geometry-optimizations and single point calculations at the B3LYP/3-21G*//B3LYP/3-21G** and B3LYP/3-21G*//MP2/3-21G** levels were performed to determine the structures and charge distributions of an enzyme substrate (1-deoxy-D-xylulose 5-phosphate) and the two inhibitors (fosmidomycin and FR-900098). The theoretically derived bond lengths are in excellent agreement with the corresponding experimental values reported for similar structures. Partial charges and dipole moments are assigned using the Mulliken and natural population analyses. The calculated structures and partial charge distributions can readily be used for the further development of biologically active inhibitors of DOXP-reductoisomerase as well as parameters for docking experiments.

Keywords DFT · Ab initio · Structure · Electrostatic potential · Antimalaria drugs

Introduction

Malaria is caused by the members of a protozoan parasite family and is transmitted by the Anopheles mosquito. It leads to death in 5–35% of severe infections and it is estimated that every year around one million children are infected with malaria. It is also a particular danger to pregnant woman leading to miscarriage or low birth weight of the child. However, it is a curable disease if promptly diagnosed and adequately treated. [1, 2] The most popular drugs are antibiotics such as tetracycline. It is often used in conjunction with other drugs to combat chloroquine resistant *Plasmodium falciparum*. Quinine and its derivatives interfere with pigment formation creating a highly toxic complex of ferriprotopophyrin–chloroquinine. Antimetabolites (antifolates) interfere with the syntheses of folic acid and DNA. Artemisine and its derivatives induce oxidant stress in the parasite. Unfortunately, rapidly developing drug resistance diminishes the efficacy of these compounds in treating new malaria cases. Despite the economic implications of malaria, so far no active anti-malaria vaccine or cheap drug based on systematic scientific studies of *Plasmodium falciparum* has been developed. It has been shown that the biosynthesis of isoprenoids depends on the condensation of a few isopentyl diphosphate units, [3] which are synthesized, in mammals and fungi, from mevalonate, which in turn is synthesized from 3-hydroxy-3-methylglutaryl coenzyme A (HMG-CoA). An attempt has been made to use 3-hydroxy-3-methylglutaryl coenzyme-A (HMH-CoA) reductase in anti-malarial drug development, but unfortunately it failed, suggesting the absence of a mevalonate pathway in *Plasmodium falciparum* [4]. An alternative pathway of isopentyl diphosphate synthesis, the 1-deoxy-D-xylulose 5-phosphate (DOXP) pathway, was recently described. [5] Here pyruvate and glyceraldehydes-3-phosphate are converted to 2-C-methyl-D-erythritol-4-phosphate with the intermediate stage of 1-deoxy-D-xylulose-5-phosphate, by the two enzymes DOXP-synthase and DOXP-reductoisomerase. The same pathway was described previously for algae and higher plants. The enzymes of the DOXP pathway are associated with the apicoplast [6, 7, 8] and this organelle could be used as a potential drug target in apicomplexan parasites. [9]

Recent studies show [10] that two phosphonate compounds fosmidomycin (FOSM) and FR-900098

Electronic supplementary material to this paper can be obtained by using the Springer LINK server located at http://dx.doi.org/10.1007/s00894-001-0053-x

I.Z. Zubrzycki (✉) · G.L. Blatch
Department of Biochemistry and Microbiology,
Rhodes University, Grahamstown 6140, South Africa
e-mail: i.zubrzycki @ru.ac.za
Tel.: +27-46-6038081, Fax: +27-46-6223984

(Fujisawa Pharmaceuticals) when given orally were able to inhibit growth of *Plasmodium falciparum*. Unfortunately, it became obvious that the half-life of these drugs is very short (tests on animal models – mice), [11] limiting significantly the practical application of these two compounds as clinical drugs. The positive feature of these two compounds is their low toxicity. One can use these two compounds as a starting point in the search for new anti-malaria drugs. In order to understand the physics of inhibitor–enzyme interactions of DOXP-reductoisomerase, an accurate description of the physical properties of the substrate as well as known inhibitors is envisaged. Thus in the presented study we investigate the structure as well as electrostatic properties of its substrate DOXP and the two inhibitors FOSM and FR-900098.

Methods

All calculations were performed on a Dell 420 Precision Station with 512 MB RAM and two processors 733 MHz each using the program Q-Chem. [12] The structures were built using the program HyperChem v.6 [13] using its internal model building procedure. Prior to submitting to the geometry optimization in Q-Chem the structures were pre-optimized using the PM3 [14] semiempirical method. The ab initio calculations of DOXP, FOSM, and FR-900098 were performed using the restricted hybrid HF-DFT SCF approach – B3LYP/3-21G*//B3LYP/3-21G** [15, 16, 17, 18] with the exchange of 0.2000 Hartree–Fock+0.0800 Slater+0.7200 Becke, and correlation 0.8100 LYP+0.1900 VWN1RPA. All calculations were performed using Pulay DIIS extrapolation. [19] The self-consistent field (SCF) converged when the Direct Inversion in the Iterative Subspace (DIIS) error was below 1.0E–08. Charges as well as orbital analyses were performed using the Natural Bond Orbital Analysis Program. [20] Single point MP2/3-21G** calculations as well as the Frontier Molecular Orbital (FMO) analysis were performed using the program HyperChem.

Results and discussion

Structural parameters characteristic for the geometry optimized B3LYP/3-21G*//B3LYP/3-21G** of DOXP, FOSM, and FR-900098 are listed in Table 1 and the optimized structures as well as the potential mapped on the surface of the molecule are shown in Fig. 1a–c. For ease of data comparison and analysis some bond lengths were averaged within groups. The atom numbering for each molecule is shown in Fig. 2a–c. Thus, the average C–H bond lengths for the CH_3 groups of DOXP and FR-900098 are 1.097 and 1.094 Å, respectively. These values are in very good agreement with the experimentally derived C–H bond length within the CH_3 group of acetone. [21] The C=O, ketone, [21] bond length present in DOXP and FOSM is also in excellent agreement with experimental results: 1.222, 1.230, and 1.213 Å for DOXP, FOSM, and experimentally derived data for $(CH_3)_2CO$, respectively. The aliphatic C–C bonds lengths within FOSM and FR-900098 are nearly the same and are on the order of 1.534 and 1.535 Å, fitting extremely well to those obtained experimentally for butane (1.531 Å). [21] A general comparison of the bonds lengths (Fig. 3) shows excellent agreement between theoretically and experimentally derived values.

To assess the possible places of “hard” and “soft” nucleophilic and electrophilic attack, analyses of the charge distribution as well as the highest occupied (HOMO) and lowest unoccupied molecular orbitals (LUMO) were performed.

To elucidate the physical properties of the molecules investigated, a natural bond orbital (NBO) analysis of charge densities and bond properties was performed. The charges and dipole moments resulting from (natural population analysis) NPA and Mulliken population analyses are collected in Table 2, Table 3, and Table 4. In order to analyze the data compiled in these tables, the main active groups had to be defined. Thus, for the DOXP molecule the two active groups consisting of O_4–P (head group) and C_2–O1, and C_3(H)OH (tail group) atoms were defined. For FOSM and FR-900098, these groups

Table 1 Comparison of computationally and experimentally derived distances (* lack of experimental reference)

DOXP		Experiment	FOSM		Experiment	FR-900098		Experiment
Atoms	Distance (Å)		Atoms	Distance (Å)		Atoms	Distance (Å)	
$CH_{3ave.}$[a]	1.097459	1.103	C–H	1.10225	1.125	$CH_{3ave.}$[a]	1.093873	1.103
C=O	1.221625	1.213	C=O	1.23036	1.212	C–C=O	1.51535	1.520
$C–C_{(ket)}$[b]	1.52325	1.520	C–N	1.35018	1.368	$C–O_{tail}$[c]	1.23605	1.213
$C–C_{(al)}$[d]	1.53435	1.531	N–O	1.40227	1.41	C1–N2	1.36326	1.368
$C–H_{(alcohol)}$	1.09927	1.10	$O–H_{(tail)}$[c]	0.987539	0.96	N2–O7	1.40807	1.41
$C–O_{(alcohol)}$	1.43569	1.431	N–C	1.44436	*	$O–H_{(tail)}$[c]	0.989487	0.96
$O–H_{(alcohol)}$	0.973504	0.971	$C–H_{(al)}$[d]	1.096025	1.117	$C–H_{(al)}$[d]	1.096087	1.117
$C–O_{(Head)}$[e]	1.40967	*	$C–C_{(al)}$[d]	1.5362	1.531	$C–C_{(al)}$[d]	1.53532	1.531
O–P	1.70464	*	C–P	1.81261	*	C–P	1.81192	*
			P–O	1.62925	*	P–O	1.629425	*
			P=O	1.48606	*	P=O	1.48662	*
			$O–H_{(Head)}$[e]	0.972416	0.971	$O–H_{(Head)}$[e]	0.972171	0.971

[a] Average; [b] Ketone; [c] Tail group; [d] Aliphatic; [e] Head group

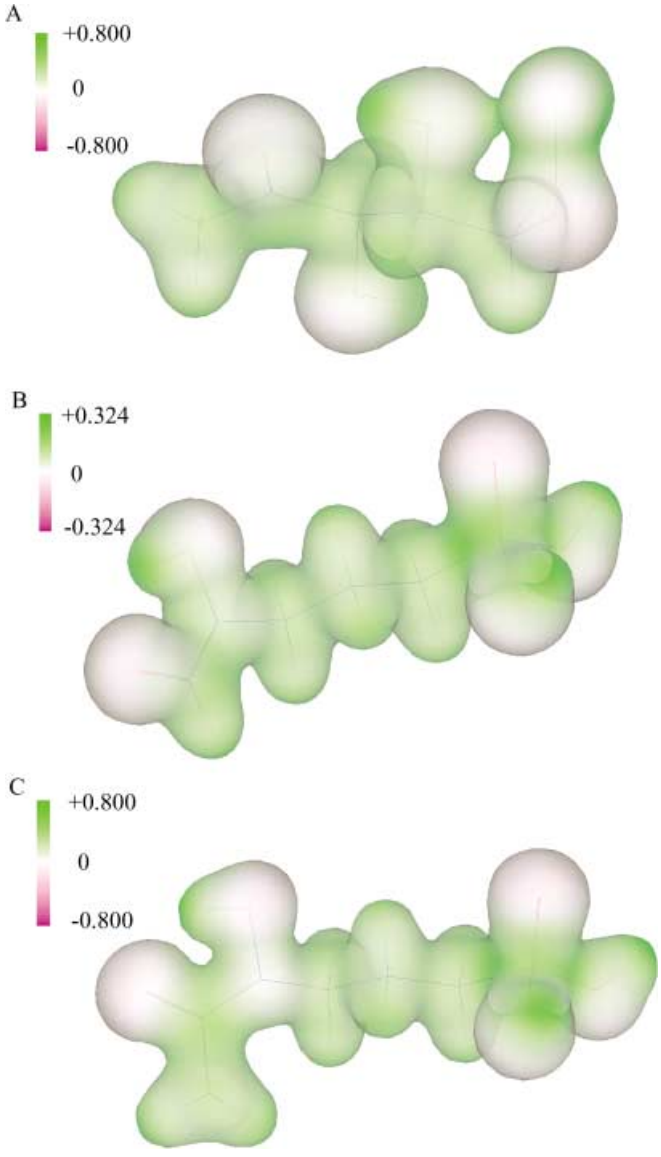

Fig. 1 Geometry optimized structures (stick representation) with the electrostatic potential mapped on the isosurface: (**A**) DOXP, (**B**) FOSM, and (**C**) FR-900098 molecules

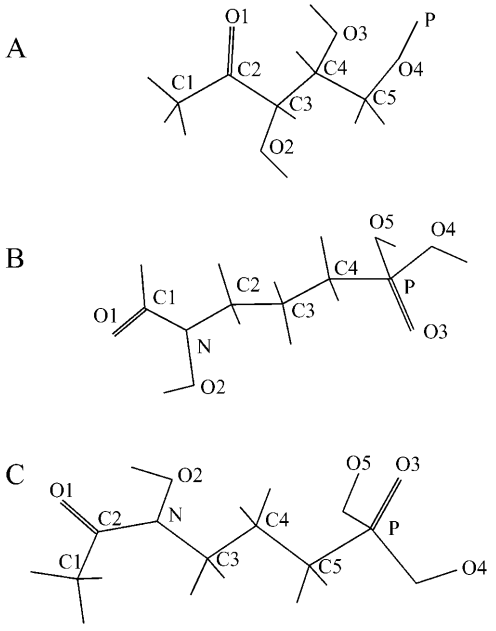

Fig. 2 Stick representation and atom numbering of (**A**) DOXP, (**B**) FOSM, and (**C**) FR-900098 molecules

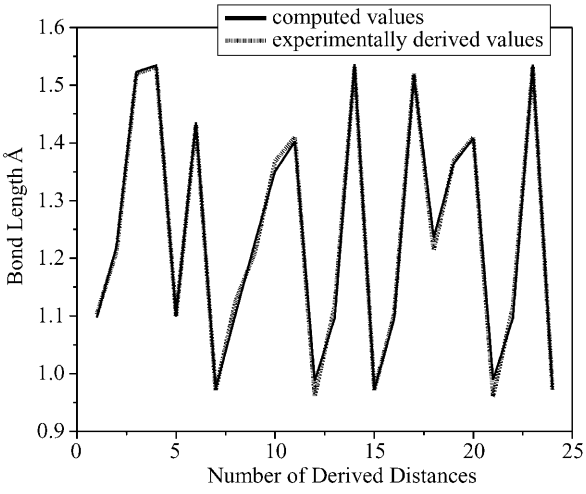

Fig. 3 Comparison of computed and experimentally derived bonds lengths

consist of P, O_3, O_4, H_{O4}, O_5, and H_{O5} (head group) for both FOSM and FR-900098 and C_1, O_1, N, and O_2, and C_2, O_1, N, and O_2 atoms for FOSM and FR-900098, respectively. The charge of the head group of DOXP is equal to –0.213, whereas for FOSM and FR-900098 it is of opposite sign and is equal to 0.053 and 0.025. The analysis of the tail groups shows that all groups have the same sign and are equal to –0.0482, –0.039, and –0.046 for DOXP, FOSM, and FR-900098 respectively. The dipole moments of DOXP, FOSM, and FR-900098 are in the range of 7–10 Debye (D). The DOXP-reductoisomerase enzyme that transforms the DOXP molecule into 2-C-methyl-D-erythritol-4-phosphate cleaves the $C_{(1)}H_3$ group and reduces the C_2–O_1 group to C–OH. Thus, the inhibiting properties of FOSM and FR-900098 are due to the physical properties of the tail groups of these two compounds. Therefore, it seems obvious that the tail groups of DOXP, FOSM as well as FR-900098 should be systematically examined. The σ_{C1C2} bond within the DOXP molecule is formed from an $sp^{2.76}$ hybrid on C_1 interacting with $sp^{1.76}$ hybrid on C_2:

$$\sigma_{C1C2} = 0.7118(sp^{2.76})_{C1} + 0.7024(sp^{1.76})_{C2}$$

corresponding roughly to the concept of interacting sp^3 and sp^2 hybrids with nearly the same electronegativity for both atoms. The analysis of the C_2–O_1 bond shows a well-localized σ_{C2O1} (1.99628e) and high occupancy π_{C2O1} bond (1.98941e) with corresponding π^*_{C2O1} antibond (0.08311e). Both the σ_{C2O1} and π_{C2O1} have slight

Table 2 Partial charges and total dipolar moment (Debye) obtained from single point (SP) Mulliken (MP2/3-21G** and B3LYP/3-21G**) and natural population analysis (NPA) (B3LYP/3-21G**) of DOXP molecule

Atom	Mulliken SP (MP2/3-21G**)	Mulliken SP (B3LYP/3-21G**)	NPA
C_1	–0.3811	–0.379	–0.784
H_{Cl}	0.168	0.142	0.263
HCl	0.151	0.135	0.261
H_{Cl}	0.186	0.163	0.279
C_2	0.509	0.433	0.596
O_1	–0.579	–0.456	–0.563
C_3	–0.564	–0.541	–0.760
H_{O2}	0.288	0.326	0.497
H_{C3}	0.186	0.135	0.248
C_4	0.094	0.127	0.032
H_{C4}	0.190	0.132	0.247
O_3	–0.597	–0.541	–0.743
H_{O3}	0.350	0.362	0.547
C_5	0.118	0.058	–0.219
H_{C5}	0.143	0.110	0.232
H_{C5}	0.123	0.099	0.213
O_4	–0.704	–0.545	–0.776
P	0.267	0.152	0.350
Tot Dip	6.03	5.94	9.98

Table 3 Partial charges and total dipolar moment (Debye) obtained from single point (SP) Mulliken (MP2/3-21G** and B3LYP/3-21G**) and natural population analysis (NPA) (B3LYP/3-21G**) of FOSM molecule

Atom	Mulliken SP (MP2/3-21G**)	Mulliken SP (B3LYP/3-21G**)	NPA
C_1	0.735	0.405	0.464
H_{Cl}	0.136	0.089	0.167
O_t	–0.643	–0.510	–0.639
N	–0.576	–0.147	–0.149
O_2	–0.382	–0.432	–0.585
H_{O2}	0.328	0.343	0.508
C_2	0.080	–0.051	–0.272
H_{C2}	0.138	0.120	0.246
H_{C2}	0.170	0.132	0.249
C_3	–0.312	–0.199	–0.488
H_{C3}	0.194	0.161	0.270
H_{C3}	0.155	0.126	0.251
C_4	–0.639	–0.394	–0.886
H_{C4}	0.175	0.150	0.274
H_{C4}	0.170	0.148	0.274
P	1.531	1.053	2.396
O_3	–0.643	–0.558	–1.078
O_4	–0.622	–0.564	–1.027
H_{O4}	0.313	0.349	0.528
O_5	–0.620	–0.568	–1.029
H_{O5}	0.312	0.348	0.528
Tot Dip	4.37	4.00	7.57

admixtures of *d* character (<0.17%). The C_2–C_3 bonds show the presence of a localized two-center σ bond with virtually the same electronegativity for both atoms. The analysis of the active tail group (C_1, O_1, N, O_2, H atoms) of the FOSM molecule shows the presence of a two-center σ_{C1-N} bond:

$$\sigma_{C1N} = 0.6013(sp^{2.15})_{C1} + 0.7991(sp^{1.51})_N$$

Table 4 Partial charges and total dipolar moment (Debye) obtained from single point (SP) Mulliken (MP2/3-21G** and B3LYP/3-21G**) and natural population analysis (NPA) (B3LYP/3-21G**) of FR-900098 molecule

Atom	Mulliken SP (MP2/3-21G**)	Mulliken SP (B3LYP/3-21G**)	NPA
C_1	–0.402	–0.400	–0.778
H_{C1}	0.186	0.154	0.275
H_{C1}	0.164	0.139	0.257
H_{C1}	0.154	0.131	0.250
C_2	0.806	0.565	0.658
O_1	–0.657	–0.542	–0.647
N	–0.582	–0.194	–0.155
O_2	–0.391	–0.441	–0.595
H_{O2}	0.331	0.343	0.509
C_3	0.073	–0.039	–0.268
H_{C3}	0.140	0.115	0.242
H_{C3}	0.158	0.125	0.241
C_4	–0.300	–0.200	–0.484
H_{C4}	0.194	0.160	0.270
H_{C4}	0.159	0.126	0.251
C_5	–0.642	–0.395	–0.886
H_{C5}	0.172	0.147	0.272
H_{C5}	0.169	0.148	0.274
P	1.530	1.053	2.396
O_3	–0.644	–0.560	–1.079
O_4	–0.622	–0.563	–1.027
H_{O4}	0.312	0.348	0.527
O_5	–0.620	–0.569	–1.030
H_{O5}	0.312	0.347	0.528
Tot Dip	4.65	4.23	8.00

with high electronegativity on N. The analysis of the C_1–O_1 bond shows the presence of localized σ_{C1O1} and π_{C1O1} bonds –1.99724e and 1.99415e, respectively with an electronegativity shift towards the O_1 atom and admixtures of *d* character. The analysis of the N–O_2 bond shows the presence of a localized two-center σ bond with very low admixtures of *d* character:

$$\sigma_{C1N} = 0.6013(sp^{2.15})_{C1} + 0.7991(sp^{1.51})_N$$

The analysis of the tail group of the FR-900098 shows a well-defined σ_{C2-N} bond:

$$\sigma_{C2N} = 0.663(sp^{2.29})_{C2} + 0.7973(sp^{1.43})_N$$

with electronegativity slightly shifted to the N atom. As for the FOSM molecule the analysis of C_2–O_1 bond shows the presence of localized σ_{C1O1} and π_{C1O1} bonds, –1.99306e and 1.98924e, with an electronegativity shift toward the O_1 atom and admixtures of *d* character. The analysis of the N–O_2 bond shows the presence of a localized two-center σ bond with very low admixtures of *d* character (<28%). The analysis of the N–O_2 bond shows the presence of a localized two-center σ bond.

$$\sigma_{NO2} = 0.677(sp^{3.80}d^{0.01})_N + 0.736(sp^{4.45}d^{0.01})_O$$

A comparison of the structure/function relationships of DOXP, FOSM, and FR-900098 suggests that the intro-

duction of an N atom is one of the main reasons for the inhibitory properties of FOSM and FR-900098. A comparison of the charge distribution between C_3 and the corresponding N atom, in FOSM and FR-900098 shows a significant increment in charge density placed on the N atom. Thus, the C_3 atom in the DOXP molecule is almost neutral with a charge of –0.011, whereas the N atoms in both FOSM and FR-900098 carry charges of –0.149 and 0.195.

In order to visualize the relative soft reactivities we have used FMO theory (results from single point MP2/3-21G** calculations). It is known that the reaction of a nucleophile preferably occurs at positions with the largest LUMO coefficient, whereas reactions of electrophiles occur at positions with the largest HOMO coefficient. Analysis of the LUMO contour map of DOXP indicates the following order $P>O_3>C_3>C_2>O_4>O_1>C_4>O_2>C_5>C_1$ of the most probable place for "soft" nucleophilic attack. In the case of a charge-controlled reaction ("hard nucleophilic attack") the probability order is $C_2>P$. A LUMO analysis of the FOSM molecule shows the largest coefficients on O_1 and N followed by $C_3>C_2>P>O_5>O_3>C_4>O_4>O_2>C_1$ and the highest positive charge on P and C_1. An analysis of FR-900098 shows the highest LUMO coefficients for O_1 and N followed by P, O_4, C_3, O_3, O_5, O_2, C_4, C_1, and C_2, whereas the largest positive charge is placed on the P atom.

Analysis of these results shows that "hard" and "soft" nucleophilic attack may occur at the opposite groups, i.e. tail for "hard" and head for "soft" attack.

HOMO analysis of the DOXP molecule shows the lowest coefficient placed at the O_4 atom with the following order of "soft" electrophilic attack $O_4>O_3>C_3>C_2>C_1>O_1>O_2>C_4>C_5>P$, whereas "hard" electrophilic attack presumably occurs at the following atoms: C_1, O_1, O_2. An analysis of FOSM shows the HOMO with the lowest coefficient placed on N atom followed by $C_4>C_3>P>C_1>O_5>O_3>O_4>C_2>O_1>O_2$. The most negatively charged atoms are O_1, O_2, and C_2. For the FR-900098 molecule the lowest HOMO coefficient are placed on the atoms in the following order: O_2<O_1<C_3<O_3<C_5<C_1<P<O_4<O_5<C_2<C_4<N, whereas the charges are distributed as follows: $O_1>N>O_2>C_3>C_4>C_5>O_3>O_4$, and O_5. Similarly to the LUMO analysis, the placement of "hard" and "soft" electrophilic attack is at the opposite ends of FR-900098.

In order to validate the steric differences between these three molecules the root mean square deviation for "backbone" heavy atoms was calculated, Fig. 4. It resulted in RMS errors of 0.366 Å between DOXP and FOSM, and 0.226 Å between DOXP and FR-900098. The calculation of volumes using grid methods described by Bodor et al. [22] resulted in the following values for DOXP, FOSM, and FR-900098: 457.57, 523.76, and 573.7 $Å^3$. Thus, the enzyme cavity accommodating the substrate or inhibitor should be in the order of 600 $Å^3$. Thus, the conclusion can be drawn that the introduction of the nitrogen atom carrying significant negative charge as compared to the carbon atom influences the molecular environment of active residues in the active center of the enzyme. Most probably this charge is able to change the three-dimensional microstructure of the active pocket of the enzyme and competitively bind to the active residue.

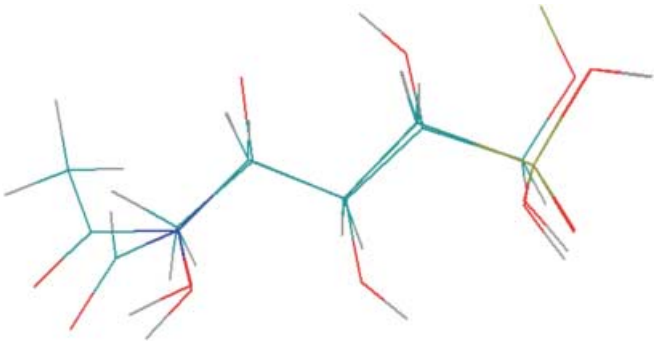

Fig. 4 Superposition of the "backbone" heavy atoms of DOXP, FOSM, and FR-900098 molecules

Supporting information available. The Cartesian coordinates and HyperChem "hin" files of the calculated structures are available as supplementary material or on request.

Acknowledgement We would like to acknowledge the financial support from Joint Research Committee (JRC), Rhodes University, South Africa, awarded to IZZ and a Wellcome Trust Tropical Projects Grant (No. 052538) awarded to GLB.

References

1. van der Werff ten Bosch JE, Demanet C, Balduck N, Bakkus MH, De Raeve H, Desprechins B, Otten J, Thielemans K (1998) Br J Haematol 102:578
2. Schlagenhauf P, Steffen R (1994) J Trop Med Hyg 97:151
3. Beytia ED, Porter JW (1976) Annu Rev Biochem 45:113
4. Grellier P, Valentin A, Millerioux V, Schrevel J, Rigomier D (1994) Antimicrob Agents Chemother 38:1144
5. Disch A, Schwender J, Muller C, Lichtenthaler HK, Rohmer M (1998) Biochem J 333:381
6. Wilson RJ, Denny PW, Preiser PR, Rangachari K, Roberts K, Roy A, Whyte A, Strath M, Moore DJ, Moore PW, Williamson DH (1996) J Mol Biol 261:155
7. McFadden GI, Reith ME, Munholland J, Lang-Unnasch N (1996) Nature 381:482
8. Kohler S, Delwiche CF, Denny PW, Tilney LG, Webster P, Wilson RJ, Palmer JD, Roos DS (1997) Science 275:1485
9. Fichera ME, Roos DS (1997) Nature 390:407
10. Jomaa H, Wiesner J, Sanderbrand S, Altincicek B, Weidemeyer C, Hintz M, Turbachova I, Eberl M, Zeidler J, Lichtenthaler HK, Soldati D, Beck E (1999) Science 285:1573
11. Murakawa T, Sakamoto H, Fukada S, Konishi T, Nishida M (1982) Antimicrob Agents Chemother 21:224
12. Kong J, White CA, Krylov AI, Sherrill CD, Adamson RD, Furlani TR, Lee MS, Lee AM, Gwaltney SR, Adams TR, Ochsenfeld C, Gilbert ATB, Kedziora GS, Rassolov VA, Maurice DR, Nair N, Shao Y, Besley NA, Maslen PE, Dombroski JP, Daschel H, Zhang W, Korambath PP, Baker J, Byrd EFC, Van Voorhis T, Oumi M, Hirata S, Hsu CP, Ishikawa N, Florian J, Warshel A, Johnson BG, Gill PM, Head-Gordon M, Pople JA (2000) J Comput Chem 21:1532

13. Hypercube (1996) HyperChem for Windows. Hypercube Inc
14. Stewart JJP (1991) J Comput Chem 12:320
15. Becke AD (1993) J Chem Phys 98:5648
16. Gordon MS, Binkley JS, Pople JA, J. PW, Hehre WJ (1982) J Am Chem Soc 104:2797
17. Dobbs KD, Hehre WJ (1986) J Comput Chem 7:359
18. Pietro WJ, Francl MM, Hehre WJ, Defrees DJ, Pople JA, Binkley JS (1982) J Am Chem Soc 104:5093
19. Pulay P, Fogarasi GJ (1992) J Chem Phys 96:2856
20. Glendening ED, Badenhoop JK, Reed AE, Carpenter JE, Weinhold F (1996) NBO 4.0. Theoretical Chemistry Institute, University of Wisconsin, Madison, Wisc. USA
21. Lide DR (ed) (2000) The CRC handbook of chemistry and physics, vol. 80. CRC Press, Boca Raton, Fla.
22. Bodor N, Gabanyi C, Wong J (1989) J Am Chem Soc 111:3783